The Effect of Foaming Additives on Acrylic Acid/Acrylamide Hydrogels

Ann Pille[1], Marie-Josée Dumont[1*], Jason R Tavares[2], Ranjan Roy[3]

[1]CREPEC, Bioresource Engineering Department, McGill University, 21111 Lakeshore Rd., Ste-Anne-de-Bellevue, Québec H9X 3V9, Canada

[2]CREPEC, Department of Chemical Engineering, Polytechnique Montréal, Montréal and Québec H3C 3A7, Canada

[3]Chemical Engineering Department, McGill University, 845 Rue Sherbrooke O, Montréal, QC H3A 0G4

[*] *Corresponding author and Page proof recipient:*

Marie-Josée Dumont, PhD.
Department of Bioresource Engineering
McGill University,
21111 Lakeshore Rd.,
Ste-Anne de Bellevue,
Québec, Canada
H9X 3V9
marie-josee.dumont@mcgill.ca

Abstract

The physical and chemical properties of hydrogels are greatly dictated by their composition. In this study, modifications were brought to the macroscopic structure of hydrogels using foaming additives, and their effects on the swelling capacity and heavy metal adsorption were investigated. Significant differences in swelling capacities were found for hydrogels synthesized with a foaming agent and a foam stabilizer (257 g/g), with a foaming agent without foam stabilizer (195 g/g), or without any additives (182 g/g). The study compared the ion removal capacity for copper (II), cadmium (II), and nickel (II) under competitive and non-competitive conditions. The use of a foaming agent significantly increased the ion removal capacity of the hydrogels, from 54 to 93 mg/g cadmium, from 75 mg/g to 104 mg/g copper, and from 48 mg/g to 80 mg/g nickel. Under competitive conditions, the hydrogels preferentially removed cadmium > copper > nickel. However, maximum removal decreased for individual heavy metals under competitive conditions.

Keywords: Hydrogels; porosity; heavy metals; swelling properties; contaminant removal

1. Introduction

Heavy metals occur naturally in the earth's crust and have a detrimental effect on human health [1]. Human activity has increased the quantity of heavy metals released into the environment. Industrial pollution, generated by various industries including agriculture, mining, and construction, is a leading source of heavy metal ions [2, 3]. The wastewater, or runoff water, from these sources contains the heavy metals and enters the water table through streams and rivers where it can come into contact with the general population if it enters groundwater. Common examples of heavy metals include cadmium, copper, lead, nickel, and zinc [4]. The maximum contaminant level in drinking water is 0.005 mg/L cadmium and 1.3 mg/L for copper [5]. The maximum tolerable soil contamination concentration of cadmium is 4 mg/kg, and 107 mg/kg for nickel [6]. Heavy metals accumulate in the body and can disrupt organ and gland function causing health problems such as organ damage, cancer, and neurological damage [1, 7-9]. Due to the adverse health effects, minimizing an individual's contact with heavy metals is essential. To do so, a possible approach is to remove them from water sources using adsorbents.

Adsorbents can be used to remove heavy metals from water. One of the most common adsorbents is activated carbon, however, can be expensive to manufacture (US$4–12/kg depending on carbon source) [10]. Low-cost adsorbents such as chitosan (US$ 15.43/kg) [11], zeolites (US$ 0.03–0.12/kg) [12], peat moss (US$ 0.023/kg) [13] and lignin (US $ 61/t) [14] have all proved to be efficient adsorbents for a variety of heavy metals (cadmium, lead, chromium, etc.) [15]. In certain cases, such as with agricultural waste adsorbents, the adsorbent must be chemically treated to activate it, thus leading to a higher environmental impact [16]. Some chemical activation methods include treatments with acids and bases [16] or the use of photo-initiated chemical vapour deposition [17]. Hydrogels are a category of adsorbent that can be used for the removal of a wide variety of heavy metals [18].

Hydrogels are 3D chemically or physically crosslinked polymeric networks that can absorb hundreds of times their weight in water. They have previously been used for soil and water remediation, namely for the removal of diesel fuel [19], motor oil [20], and a variety of heavy metals such as copper [21, 22], zinc, and nickel [18, 22]. Hydrogels can be synthesized from many different monomers, both synthetic and bio-based, the most prominent including acrylic acid and acrylamide. Acrylic acid/acrylamide hydrogels have demonstrated large swelling capacity and significant ion removal over a range of concentrations for a variety of heavy metals [23].

Acrylic acid and acrylamide can be used as monomers when synthesizing hydrogels of differing porosity. The porosity and the shape of the pores are determining factors of a hydrogel's structure and swelling ability. There are three categories of hydrogel structures: (1) non-porous hydrogels, (2) superabsorbent hydrogels, and (3) super-porous hydrogels. Previous generations of superabsorbent and super porous hydrogels were prepared in various ways, including freeze-drying [24]. Modern versions are typically prepared using the gas blowing technique (acid-induced decomposition of a foaming agent) and by the use of a foam stabilizer [25]. Non-porous hydrogels are synthesized without any additives, and superabsorbent hydrogels are synthesized using only a foaming agent [26]. Non-porous hydrogels are solid and rigid with no porous network. The average pore size is under 10 nm, and they are non-continuous. They generally have a slow swelling rate [27]. Superabsorbent hydrogels typically form a solid, flexible, unstable foam [27]. They have a micro to macroporous pore structure and pore sizes ranging from 10 nm - 1µm. The swelling rate of superabsorbent hydrogels depends on the porosity of the individual sample [27]. Super porous hydrogels form a solid, flexible, stable foam with an open-cell structure and pore sizing over 1µm [27]. They have a rapid swelling rate, and previous acrylic acid/acrylamide hydrogels produced using the gas blowing technique have reported swelling capacities of 159 g/g [28] and 194 g/g [29]. In this study, the hydrogels will be referred to by their additives. The hydrogel without any additives will be referred to as the base hydrogel (BH), the hydrogel with a foaming agent as the foaming agent hydrogel (FAH), and the hydrogel with both a foaming agent and a foam stabilizer as the foaming agent, foam stabilized hydrogel (FAFSH).

Previous research work on the synthesis of acrylic acid/acrylamide super porous hydrogels focused on the effect of crosslinker and foaming agent concentration, as well as their mechanical properties. This work reports, for the first time, a systematic comparison of the properties of three hydrogel structures synthesized using the same monomers. The impact of the porosity of the hydrogels on the swelling ratio, and the adsorption of heavy metals (copper (II), nickel (II), and cadmium (II)) under competitive and non-competitive conditions has been studied.

2. Materials and Methods

2.1 Materials

Acrylic acid (AA) (99% purity), acrylamide (AM) (99% purity), N, N'-methylenebisacrylamide (NMBA) (99% of purity), Pluronic F127, ammonium persulfate (APS)

(98% purity), N,N,N', N'-tetramethylethylenediamine (TEMED) (99% purity), sodium hydroxide (NaOH) (98% purity), sodium bicarbonate ($NaHCO_3$) (99% purity), copper sulfate (99% purity), nickel chloride (98% purity) and cadmium chloride (99.99% purity) were purchased from Sigma-Aldrich Co. LLC, USA. Ethanol (purity of 95%) and nitric acid (86% purity) were purchased from Fisher Scientific (Fair Lawn, NJ, USA). Distilled water (DW) with a resistance of 18 megaohms/cm ^{2} was used in all preparations and tests.

2.2 Hydrogel Synthesis

In a typical experiment, 5 g AM was dissolved in 10 ml DW and mixed with 5 ml AA. The pH of the solution was adjusted to 5.5 using 5M aqueous NaOH. The pH-adjusted solution was then used to make 1 of 3 structures:

1. the base hydrogel (BH): 0.05 g NMBA was added to the AA/AM pH adjusted solution and stirred at 300 rpm and 70 °C in an oil bath for at least 10 minutes or until dissolved. Afterward, 2 ml of a 10 (w/v) % APS solution was added and stirred for 1 minute. Finally, the stir bar was removed, and 2 ml TEMED was added to the solution and stirred quickly with a spatula. The reaction was allowed to proceed for 5 minutes at 70 °C, and the hydrogel was dried.
2. The foaming agent hydrogel (FAH): 0.05 g NMBA was added to the AA/AM pH-adjusted solution and stirred at 300 rpm and 70 °C in an oil bath for at least 10 minutes or until dissolved. Afterward, 2 ml of a 10 (w/v) % ammonium persulphate solution was added and stirred for 1 minute. Following this, 0.5 g of foaming agent ($NaHCO_3$) was added to the solution and mixed for 20 seconds. Finally, the stir bar was removed, and 2 ml TEMED was added to the solution and stirred quickly with a spatula. The reaction was allowed to proceed for 5 minutes at 70 °C, and the hydrogel was dried.
3. The foaming agent and foam stabilizer hydrogel (FAFSH): 0.05 g NMBA and 1 g of foam stabilizer (Pluronic F127) were added to the AA/AM pH adjusted solution and stirred at 300 rpm and 70 °C in an oil bath for at least 10 minutes or until dissolved. Afterward, 2 ml of a 10 (w/v) % ammonium persulphate solution was added and stirred for 1 minute. Following this, 0.5 g of $NaHCO_3$ was added to the solution and mixed for 20 seconds. Finally, the stir bar was removed, and 2 ml TEMED was added to the

solution and stirred quickly with a spatula. The reaction was allowed to proceed for 5 minutes at 70 °C, and the hydrogel was dried.

Hydrogels were dried using one of two methods: freeze-drying or oven drying. To prepare hydrogels for the drying process, they were cut into small pieces and then rinsed with a 50/50 solution of ethanol and distilled water until the solution ran clear. After the rinsing process, hydrogels that were freeze-dried were frozen at -15 °C for 16 hours. The hydrogels were freeze-dried (Labconco, FreeZone 2.5) under vacuum at -46 °C for 48 hours. After the rinsing process, hydrogels that were oven-dried were immersed in ethanol for 24 hours. The samples were then put in an oven (Precision Scientific, Thelco Laboratory Oven) for 72 hours at 70 °C. After drying, all hydrogels were ground into a powder using a Black & Decker CBG110SC Grinder and stored in a desiccator.

2.3 Morphology

The macroscopic structure of the hydrogels was observed using images of the hydrogel taken before the drying process. The morphologies of the original and regenerated hydrogels were studied using a scanning electron microscope (SEM) (SU3500, Hitachi High-Technologies Co., Tokyo, Japan) at 1000x magnification at an acceleration voltage of 10 kV, beam current of 140 µA and a working distance of 5700 µm.

2.4 Surface Area

The BET (Brunauer, Emmett, and Teller) surface area, BJH (Barret, Joyner, and Halenda) adsorption cumulative surface area, and single point surface area data were obtained with BET surface area analysis performed by a nitrogen adsorption-desorption apparatus (TriStar 3000, Micromeritics Co., USA). Each sample weighed approximately 1 g and had been degassed for 20 hours at 120 °C prior to the test.

2.5 Swelling Measurements

The swelling tests were performed with 6 replicates as follows: nylon tea bags were initially weighed (m_1). The tea bags were immersed in water for 2 h, after which they were removed and hung in the air for 10 min to remove the excess water. They were weighed again, and this wet bag weight was recorded (m_2). After drying the bags in an oven until constant weight, they were

weighed again (m_3). Finally, they were loaded with ≈50 mg of dry hydrogel, which was recorded as the weight of the loaded bag (m_4). The loaded tea bags were placed in excess distilled water and allowed to swell, removing them (at 0.25, 0.5, 1, 24, and 48 hrs) for weight measurements (m_x). The bags were hung for 10 minutes to allow excess water to drip off before weighing.

The weight ratio of absorbed water to the original hydrogel sample (q (g/g)) is calculated using Eq. (1).

$$q = \frac{m_x - m_4 - (m_2 - m_1)}{m_4 - m_3} \qquad (1)$$

The swelling ability of the hydrogels was tested in varying pH (2, 4, 6, 8, 10, 12) using this same tea bag method with 6 replicates.

2.6 Regeneration of Hydrogels

To observe the effect of a 24-hour distilled water wash on the swelling properties of the hydrogels, samples of the three structures were swollen in distilled water for 24 hours and then dried in an oven at 70 °C until constant mass was reached (72 hours). The hydrogels were then ground into a powder and used to test the swelling ability of regenerated hydrogels, denoted by the letter *R* (RBH, RFAH, RFAFSH) using the tea bag method with 50 mg of powdered sample and 6 replicates in distilled water and at varying pH (2, 4, 6, 8, 10, 12). Samples were swollen for 24 hours, and then the mass was recorded.

2.7 Reusability of Hydrogels

The reusability of the oven dried FAFSH AA/AM hydrogel was tested using the tea bag method with 50 mg of powdered sample in distilled water using 6 replicates. Samples were repeatedly swollen for 24 hours and then dried at 70 °C for 24 hours until the swelling ability remained relatively constant.

2.8 Metal Binding Tests

The metal binding ability of the hydrogels (original and regenerated) was determined using inductively coupled plasma-optical emission spectroscopy (ICP-OES) (Thermo 6500 Dual View, Thermo Fisher Scientific, US). The metals tested were copper, nickel, and zinc. NIST traceable standards were used to prepare the calibration curves for each metal. Trace metal grade nitric acid

(4 vol%) was used for all dilutions. The calibration curve had a range from 0 to 100 mg/L. The standard bracketing technique was used to correct for drift over time. In addition, 2 quality control points, at 0 and 10 ppm, were used to ensure the quality of the data.

For the metal adsorption tests, ≈50 mg of hydrogel powder was placed in a 50 ml aqueous solution of an individual metal (100 ppm), distilled water, or all three metals (33 ppm each) and left at room temperature without agitation for 24 h. Additionally, distilled water blanks and metal solution blanks were prepared, to perform a spike recovery study. After completing the process, the hydrogels, the blanks and the spikes were filtered using vacuum filtration followed by a second filtration using 1.0 µm DigiFilters (SCP science, Montreal). The volume of the remaining supernatant was recorded after the first filtration. The remaining solutions were analyzed using ICP-OES with a 50/50 dilution with 4% Vol trace metal grade nitric acid. The adsorption tests were performed in triplicate.

The initial concentration of the supernatants was determined using the spike for each metal solution, and the metal's removal was calculated using Eq 2:

$$Removal = \frac{(C_1V_1 - C_2V_2)}{m} \quad (2)$$

Where C_1 is the initial concentration of the ion solution, V_1 is 50 ml, C_2 is the concentration after 24 hours of hydrogel adsorption, V_2 is the volume measured after hydrogel removal, and m is the dry mass of the hydrogel.

3. Results and Discussion

3.1 Mechanism and Foam Structure

The hydrogels were synthesized by copolymerization of acrylic acid and acrylamide in the presence of NMBA, a crosslinker. The proposed mechanism for copolymerization is shown in Figure 1 [30-32]. As seen in the figure, the foaming agent and foam stabilizer used in some formulations are not part of the final hydrogel structure.

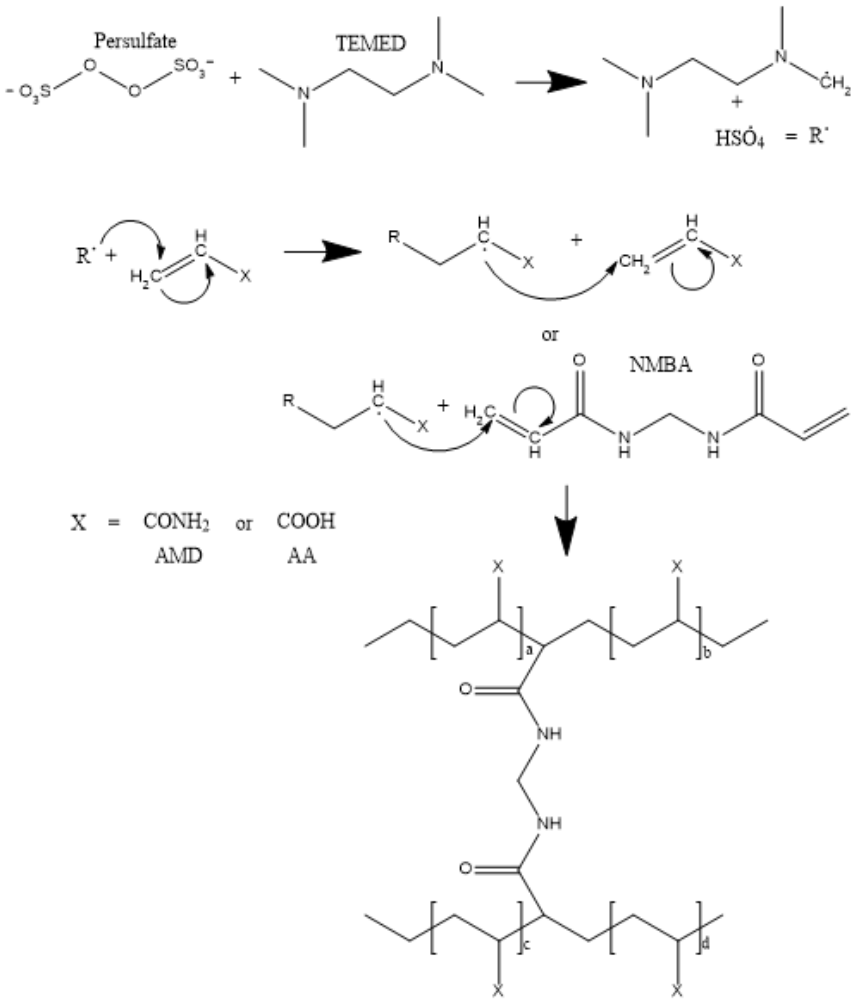

Figure 1: Mechanism of synthesis of acrylic acid/acrylamide hydrogel

APS and TEMED were used as initiators. Under heating, ammonium persulphate decomposed into ammonium and persulphate ions. The TEMED was added to increase the speed of sulfate anion-radicals formation [33]. The hydrogens from the functional groups of the acrylic acid or acrylamide were attracted to the anion radical and formed macroradicals. Thereafter, the macroradicals initiated polymerization, creating the copolymer [30]. Due to the presence of a crosslinker, the copolymer formed a three-dimensional crosslinked structure. The blowing agent reacted with acid in solution and released carbon dioxide, which caused the formation of bubbles. These bubbles were stabilized by Pluronic F-127 when the FAFSH was synthesized [29].

The ratio of acrylic acid to acrylamide in the final network was fixed at 50/50 based on swelling results taken from another study [31].

The difference in macroporous structure was evident when observing the hydrogels before the drying process (Figure 2). The BH sample had no foam structure. The hydrogel was flat and clear, with minimal bubbles caused by air escaping during synthesis. The FAH had an unstable foam structure. Many of the pores generated by the foaming agent collapsed during synthesis. The FAFSH sample was a stiff, stable foam. The foam stabilizer supported the foam structure during synthesis, which allowed the rigid hydrogel foam to form. These results were consistent with the literature [26].

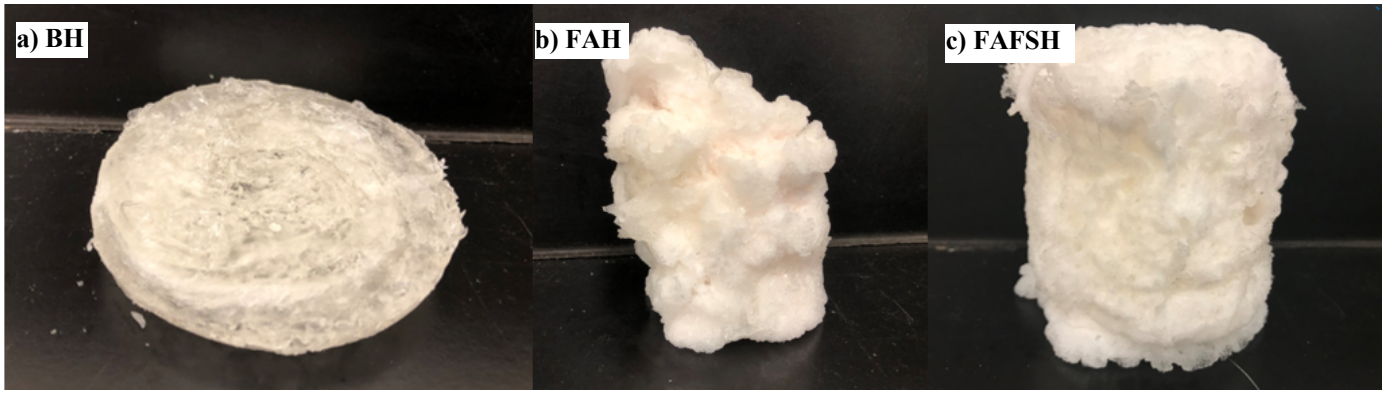

Figure 2: a) base hydrogel, b) foaming agent hydrogel, c) foaming agent, foam stabilized hydrogel

3.2 SEM

When using SEM to examine the six structures, the pores of the original hydrogel structures were apparent. As seen in Figure 3, these pores were not present in the regenerated samples. This suggested that the 24-hour distilled water wash altered the surface of the hydrogel by removing the pores. Small (<50 µm), uniform pores were present on the surface of the BH samples. This showed that while the macrostructure was not porous, the pores were still present at a microscopic level. Pores of varying sizes (> 50 µm) were present on the FAH samples. Additionally, there were fewer pores present on the FAH samples than the BH samples and they had a greater variation in shape. The FAFSH samples had a rough surface and many pores varying in both size and shape. There was a larger quantity of pores present in the FAFSH samples than the FAH samples.

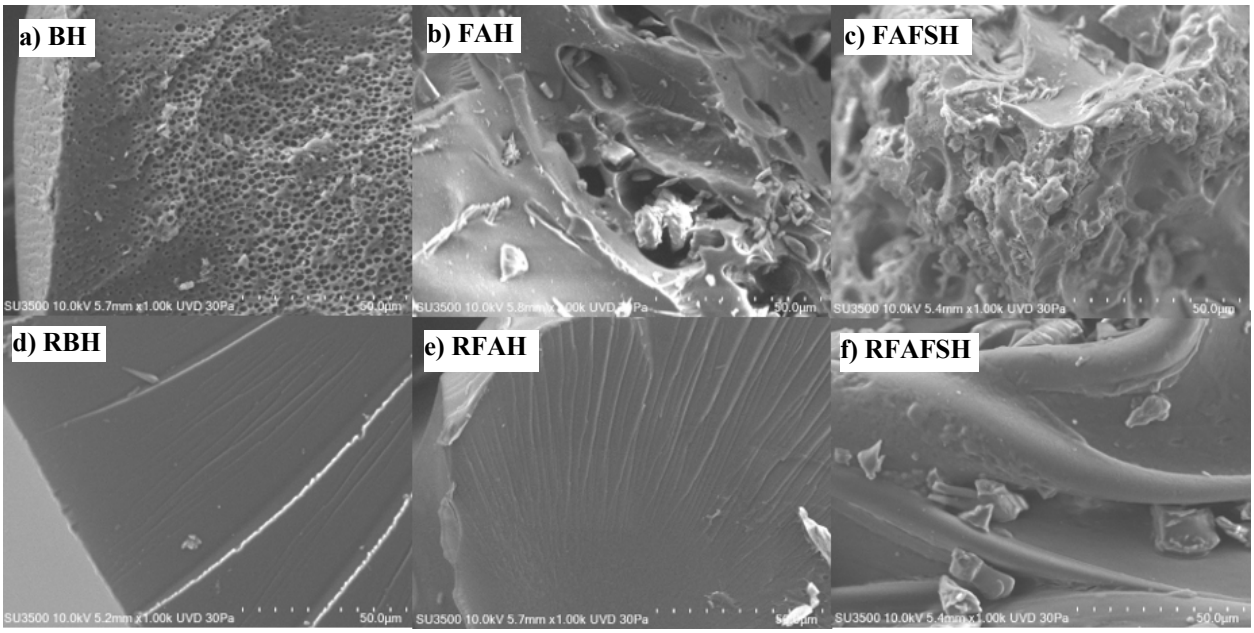

Figure 3: SEM images - 50 μm a) BH, b) FAH, c) FAFSH, d) RBH, e) RFAH, f) RFAFSH

A previous study found that the swelling capacity of hydrogels was affected by the internal pore structure rather than the surface pore structure. Minor changes in surface pore structure had a minimal effect on swelling capacity [34]. This explained why the hydrogels with the largest number of pores (BH and FAFSH) had a significant difference in swelling capacity.

3.3 Surface Area

Powdered samples were used for surface area tests, the results of which are shown in table 1. Due to the low surface area of the samples, some measurements could not be performed as they were below the detection limit. From the BET surface area measurements, the RFAH and RFAFSH samples had very low surface area values, and the instrument could not obtain a measure for the RBH sample. The low surface area measurements support the SEM data, which showed that the regenerated samples did not have surface pores.

Table 1: BET Results

Sample	Swelling Capacity (g/g)	BET Surface Area (m^2/g)	Adsorption Average Pore Width (Å)	t-Plot micropore volume (cm^3/g)
BH	182	0.0436	40.29	0.000035
FAH	195	0.0223	NA	0.000038
FAFSH	257	0.0276	NA	0.000032
RBH	219	NA	NA	NA
RFAH	204	0.001	6168.16	NA
RFAFSH	285	0.002	NA	NA

By contrast, the original samples had higher surface areas. The BH sample had the highest surface area. This supports the SEM data as pores were visible on the BH samples. The FAH and FAFSH samples had similar surface areas. When comparing the BH surface area to the FAH and FAFSH surface areas, it is obvious that while using a foaming agent did change the foam structure of the hydrogel, it did not significantly increase the porosity at a microscopic level, it simply changes the shape of the pores. This was surprising as previous literature reports that use of a foaming agent increases the porosity, and therefore surface area, of AA/AM hydrogels [27].

3.4 Swelling Ability

The hydrogel synthesis procedure was adapted from Adnan et al. [28] and Shu King et al. [29]. Oven drying was explored as it is a common way of drying hydrogels. It was compared to freeze-drying as this method tends to preserve the pore structure of dried material. Varying initiator and crosslinker concentrations were tested to determine the effect on swelling ability (Table 2).

Table 2: Hydrogel Formulations

SAMPLE	STRUCTURE	DRYING METHOD	INITIATOR (VOL%)	CROSSLINKER (VOL%)	FOAM STABILIZER (WT%)	FOAMING AGENT (WT%)
1	BH	Oven	20	0.5	0	0
2	FAH	Oven	20	0.5	0	5
3	FAFSH	Oven	20	0.5	10	5
4	FAFSH	Oven	10	0.5	10	5
5	FAFSH	Oven	20	1.5	10	5
6	FAFSH	Oven	20	2.5	10	5
7	FAFSH	Freeze-dried	10	0.5	10	5
8	FAFSH	Freeze-dried	20	0.5	10	5

The final swelling capacity was affected by crosslinker content, initiator content, drying method, and hydrogel structure. As seen in Figure 4, decreasing the crosslinker content increased the swelling capacity. This was consistent with the findings of Chavda et al., who found that an increase in crosslinker concentration led to increased crosslinking density and lower swelling capacity in super porous hydrogels [35]. However, when a crosslinker content below 0.5 wt% was used, the hydrogel was unable to form. A crosslinker concentration of 0.5 wt% NMBA was chosen as it demonstrated the highest swelling capacity at 210 g/g. Similar hydrogels reported swelling capacities of 159 g/g [28] or 194 g/g [29], however they were synthesized using 2.5% NMBA. A higher swelling capacity was achieved for the hydrogel synthesized in this study by using less crosslinker.

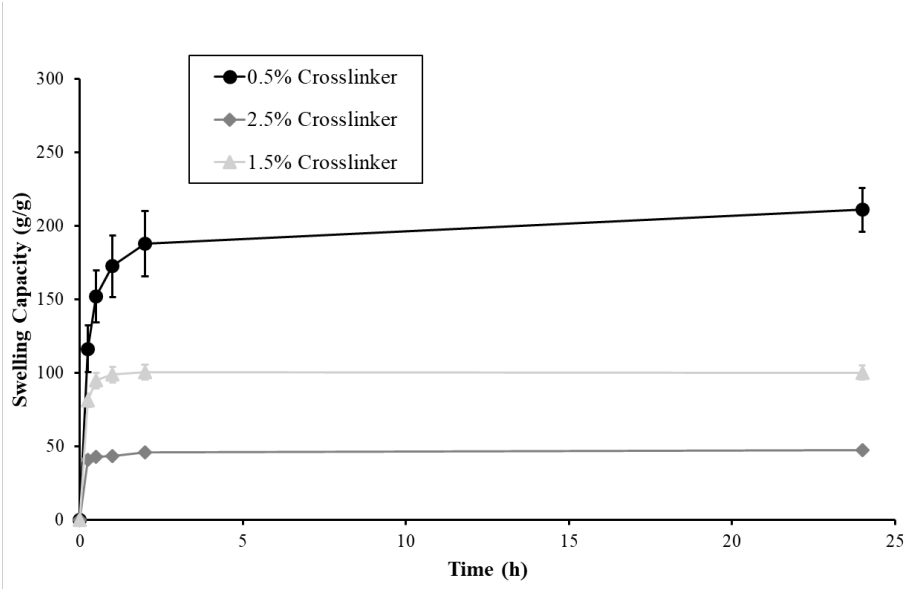

Figure 4: Swelling capacity of oven dried, foaming agent, foam stabilized hydrogels with 20 wt% initiator

The drying method and initiator concentration had a significant effect on the final swelling capacity. The two drying methods used were oven drying at 70 °C and freeze-drying at -46 °C. As seen in Figure 5, freeze-drying produced a higher swelling capacity when both 10 and 20 wt% initiator were used. This was attributed to the fact that freeze-drying preserved the porous structure. Oven drying allowed the shrinkage and collapse of the pores [36].

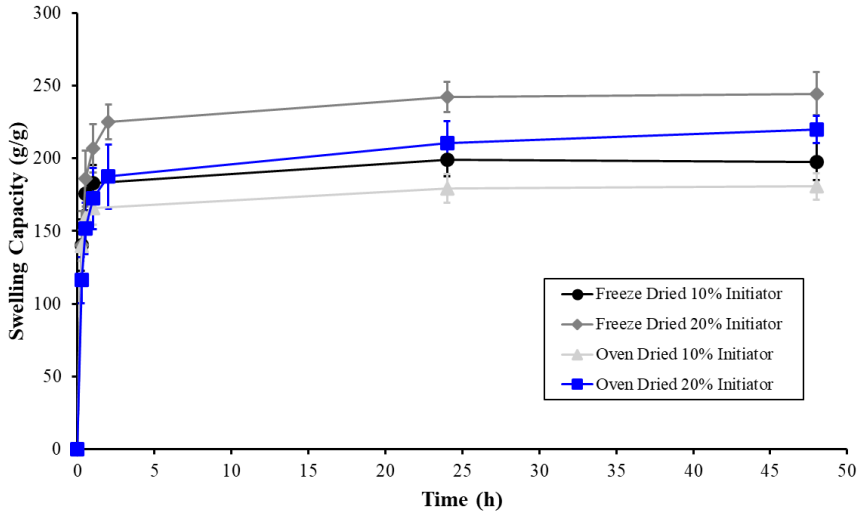

Figure 5: Swelling capacity of foaming agent, foam stabilized hydrogels with varying initiator content and drying methods

However, the freeze-dried samples do not have a significantly higher swelling capacity as the error bars overlap. Because the swelling capacity of the oven-dried and freeze-dried samples are almost identical and that the freeze-drying process is expensive [36], oven drying was selected as the drying method.

As seen in Figure 5, when the initiator concentration was reduced from 20 (wt or vol)% to 10 (wt or vol)%, the swelling capacity decreased (from 220 g/g to 181 g/g). This was observed for both freeze-dried and oven-dried samples. Due to the higher swelling capacity, 20 (wt or vol)% initiator was selected. While 20 (wt or vol)% is a very high value for initiator content, it is consistent with previous studies reporting on super porous hydrogels [28, 29]. A very fast rate of reaction is required in order to preserve the porous structure of the hydrogels. As seen in Figure 5, when less initiator is used, the rate of reaction is not sufficient, and the final swelling capacity is reduced.

The structure of the hydrogels affected their final swelling capacity and their swelling rate. As seen in Figure 6, all three structures experienced rapid swelling in the first 15 minutes (288 g/gh-472 g/gh). The swelling rate then reduced over time up to two hours, and a slow swelling rate was observed from 2 to 24 hours. The FAFSH experienced the fastest initial swelling rate. This rapid swelling capacity is a characteristic of super-porous hydrogels [27-29].

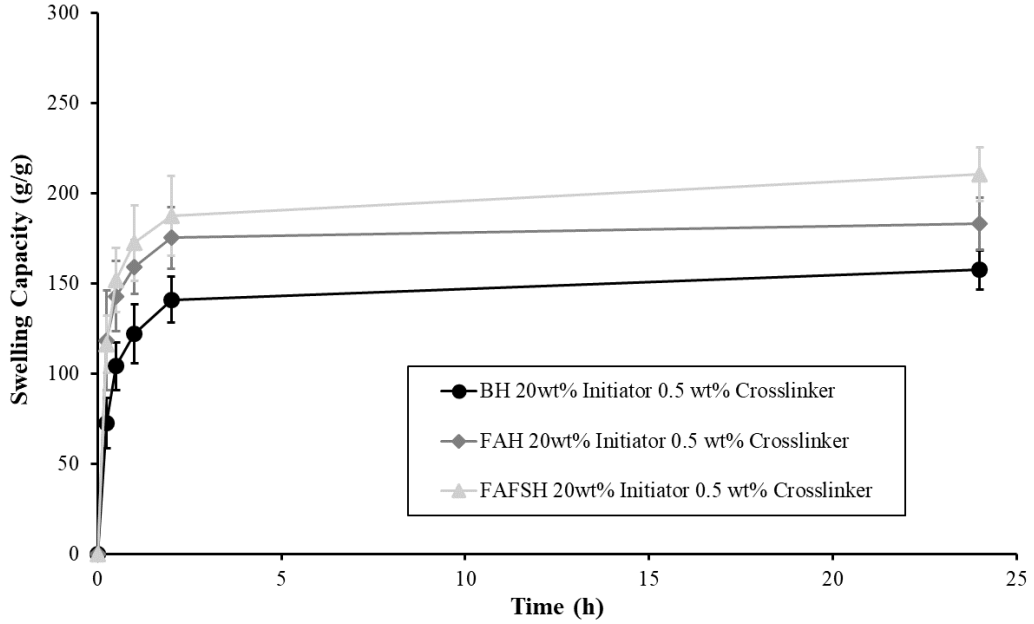

Figure 6: Swelling dynamics of acrylic acid/acrylamide hydrogel structures

In addition to affecting swelling dynamics, the structure affected the final swelling capacity. As shown in Table 3, FAFSH had the highest 48 hr swelling capacity at 256 g/g, whereas the FAH samples swelled to 195 g/g and the BH samples to 182 g/g. The difference between these swelling abilities was deemed to be significant using a single factor ANOVA (α=0.05). The swelling capacity of the FAFSH samples was higher than 159 g/g [28] or 194 g/g [29], which had previously been reported for the synthesis of similar hydrogels using a foaming agent and foam stabilizer.

Table 3: 24 h swelling capacity of hydrogel structures

Hydrogel Structure	*Swelling Capacity (g/g)*
BH	182 +/- 6
FAH	195 +/- 11
FAFSH	257 +/- 17

These swelling results are lower than those reported by other novel acrylic acid/acrylamide hydrogels or composite acrylic acid hydrogels (Table 4). However, they demonstrate that swelling capacity can be improved with the use of foam additives.

Table 4: Swelling capacity of several novel acrylic acid hydrogels

Hydrogel	*Swelling Capacity*
poly (acrylic acid-co-acrylamide) /bentonite/ kaolin composite hydrogel	Up to 600 g/g [37]
Poly (acrylic acid-co-acrylamide) hydrogel	Up to 70 000 % [38]
pH sensitive poly(acrylamide-co-acrylic acid)	Over 3000 % [39]
acrylamide–acrylic acid hydrogel	Up to 1040 % [40]

3.4.1 Effect of Regeneration

The synthesis process for most hydrogels includes a rinse in distilled water to remove unreacted components that contaminate the network. However, this step affected the structure of the original hydrogels and was therefore not included in the original procedure. As seen in Figure 7, the regenerated hydrogels had a higher swelling capacity than the original hydrogels.

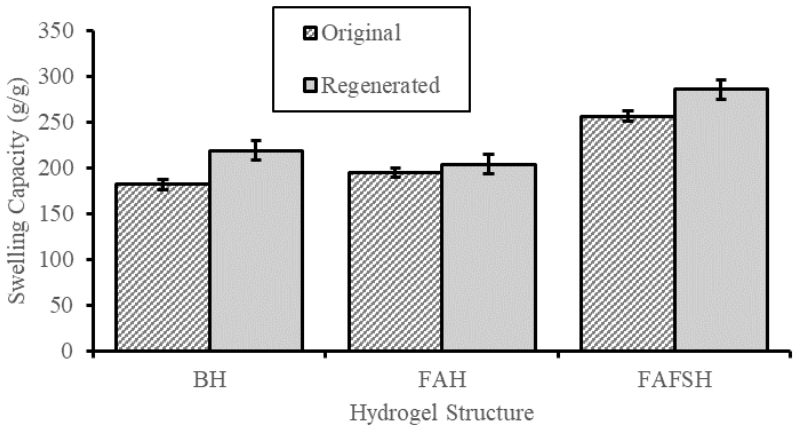

Figure 7: Original and regenerated hydrogel swelling capacity in distilled water (24 h)

This difference was found to be significant using a single factor ANOVA (alpha= 0.05). This improvement was most likely due to small amounts of unreacted reactants present in the original hydrogel matrix [22, 37].

3.4.2 Effect of pH

The swelling capacity of a hydrogel is affected by the properties of the liquid it is immersed in, including ionic strength, temperature, and pH. As pH increases or decreases from neutral, the swelling capacity of the hydrogel usually decreases [41, 42]. As seen in Figure 8a, the hydrogels had the highest swelling capacity in distilled water. The swelling capacity was slightly reduced at pH 4, 6, 8 and 10, and drastically reduced at pH 2 and 12. This is because highly acidic or basic conditions change the charge of functional groups.

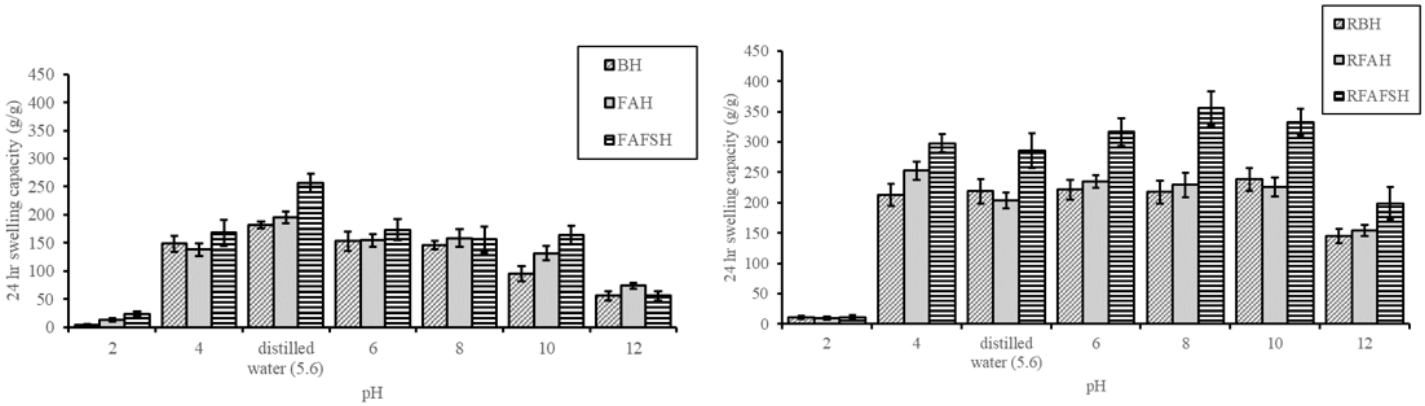

Figure 8: a) Swelling capacity of oven dried hydrogels at varying pH, b) Swelling capacity of regenerated oven dried hydrogels at varying pH

At acidic pH, carboxylate ions became protonated, which changed their charge [43]. This caused the network to shrink due to increased hydrogen bonding and new physical interactions. The shrinkage of the network decreased the swelling ability [43]. Additionally, changes in the charge of functional groups reduced the hydrogel's internal repulsion and decreased the hydrogel's swelling capacity. At medium pH, some carboxylate groups became ionized which broke the hydrogen bonds and caused repulsion between the negatively charged groups, thus increasing the swelling ability of the hydrogel [43]. At very basic pH, charge screening decreased the swelling ability. This resulted from excess Na^+ ions that prevented proper anion-anion (OH^- & OH^-) repulsion in the hydrogel [43].

The regenerated hydrogels showed high swelling capacities in basic pH. As shown in Figure 8b, the regenerated hydrogels had the highest swelling capacity at pH 8 rather than pH 5.6. Additionally, the regenerated FAFSH outperformed the BH and FAH samples by a much higher margin at pH 6 and 8 than the original samples. Finally, the regenerated samples showed higher swelling capacities than the original samples at all pHs, making them a better option for absorption in environments with varying pH.

3.5 Reusability

Reuse of a polymer that maintains its properties is more desirable than the synthesis of a new polymer. As seen in Figure 9, the swelling capacity of the three structures either increased or

stayed constant over cycles 1–3. After cycle 6 is had stabilized. The FAFSH showed the most considerable reduction in swelling capacity. However, its swelling capacity remained around 80% of initial swelling. The hydrogels show a constant swelling capacity, suggesting that the material remains stable even after multiple swelling cycles. This indicates that they would be suitable for a long-term use.

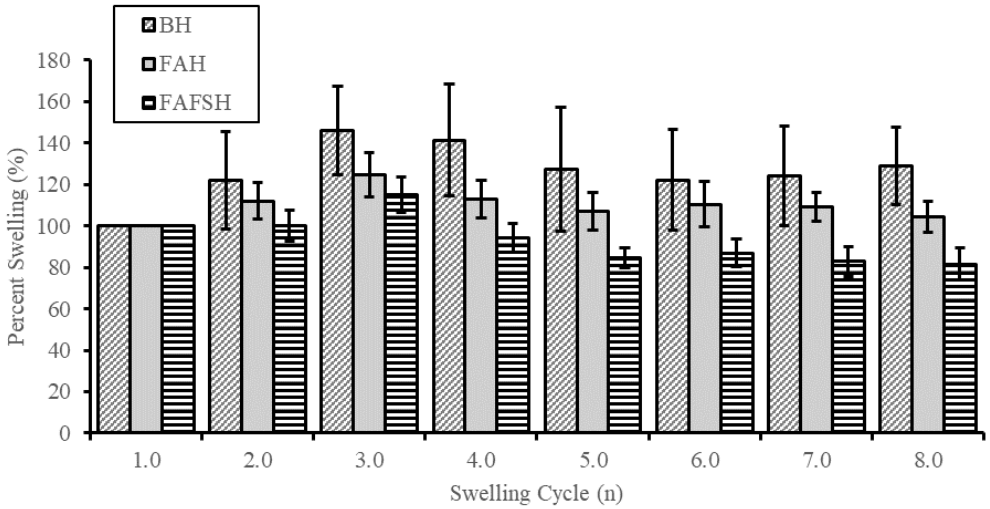

Figure 9: Reusability of oven dried hydrogels

3.6 Heavy Metal Adsorption

Heavy metal adsorption was measured using the original and regenerated hydrogels in solutions of copper (II), cadmium (II) and nickel (II) ions. These ions were chosen as they are among the most commonly found in wastewater [44] and are often used for heavy metal adsorption tests in the literature [22, 38, 45]. The data were then analyzed using multiple two-factor ANOVAs (alpha=0.05) with three replicates. It was determined that there was no statistical difference in the ion removal capacity of the original and the regenerated samples. However, the removal was affected by the hydrogel structure and the heavy metal ion. As can be seen in Figure 10, under non-competitive conditions, the removal capacities of the FAH and FSFSH hydrogels were not statistically different and were significantly larger than the removal of the BH hydrogel. The initial concentration of the ion solutions were 105 ppm (Cu), 109 ppm (Cd) and 99 ppm (Ni). The variation between the expected and the actual results for the spikes were 5%, 9% and -1%

respectively. The FAFSH samples had a removal capacity of 103.7 mg/g +/- 1.9 mg/g copper (II), 92.3 mg/g +/- 9.3 mg/g cadmium (II), and 73.2 mg/g +/- 12.6 mg/g nickel (II).

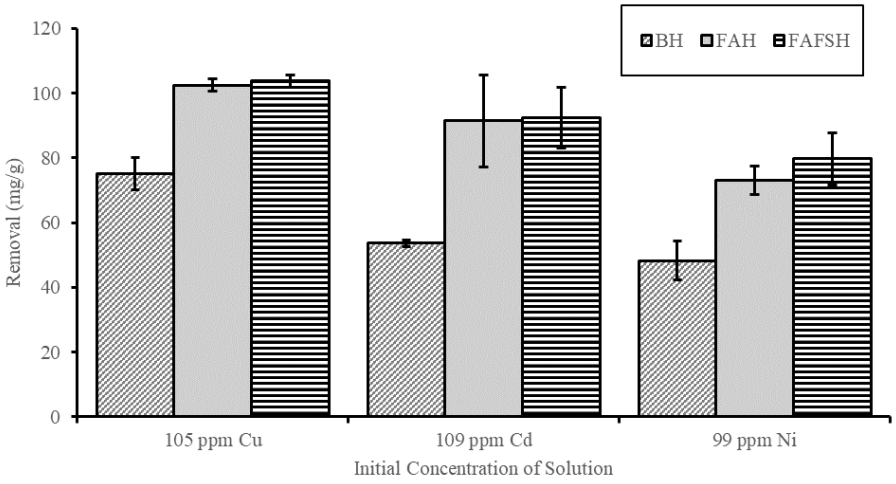

Figure 10: Heavy metal removal under non-competitive conditions (24 h)

Under competitive conditions, the structures and ions' type also affected the removal. The removal of the FAH and FAFSH were not significantly different, but the BH had a significantly lower removal capacity. As shown in Figure 11, the order of preference for removal of the hydrogel was Cd> Cu> Ni. The removal capacity for individual ions was decreased under competitive conditions. Both copper and cadmium, having a higher removal than nickel, is consistent with previous literature [46-50]. Cadmium had the highest initial concentration, which can explain the highest adsorption by the hydrogels.

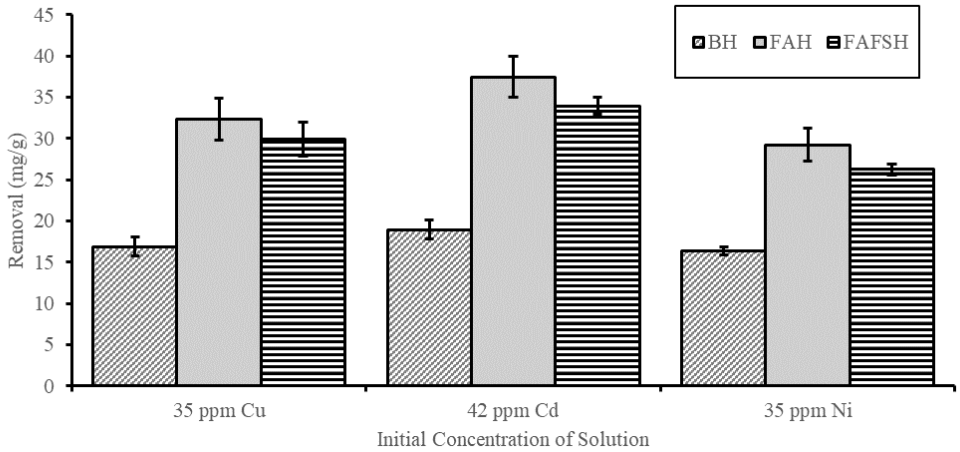

Figure 11: Heavy metal removal competitive conditions (24 h)

Heavy metals are removed from the solution through ion chelation. Functional groups such as carboxyl, amide, imidazole and pyridine can participate in the chelation reactions [51, 52]. The carboxyl and amide functional groups in acrylic acid and acrylamide are capable of forming complexes with the divalent ions [51-54] such as those used in the experiments.

The removal capacity of the hydrogels was affected by many factors, including the initial concentration of the ion solution, the pH of the solution, the ions present, and the length of time the experiment is run [55]. Therefore, it can be challenging to compare ion removal capacity as the start conditions must be similar in order to make a valid comparison. In this study, the initial concentration of the ion solution was approximately 100 ppm, the pH was around 5, and the ion solutions were in contact with the hydrogels for 24 hours.

A study performed by U. Yildiz et al. showed that the ion removal capacity of a PVP (poly N-vinyl-2-pyrrolidone) hydrogel increased in more basic start conditions [45]. PVP hydrogels were immersed in 5 ppm metal solutions for 24 hours at pH 2, 5, and 8. The highest removal efficiencies were recorded at pH 8. At pH 5, the recorded removal capacities were 75 mg/g for copper, 32 mg/g for nickel, and 12 mg/g for cadmium. The removal capacity of the PVP hydrogel was increased by incorporating other monomers into the hydrogel structure. The maximum recorded removal at pH 5 was 130 mg/g copper, 105 mg/g nickel and 40 mg/g cadmium [45]. These measures were higher than, but comparable to, the measures reported in this paper, however cadmium was removed in lower quantities in the Yildiz et al. study. Additionally, a hydrogel with similar monomers to the presented hydrogel had a maximum ion removal capacity

of 121 mg/g and was selective towards copper and zinc over other tested ions [38]. This removal capacity for the reported hydrogel was higher than the removal capacity reported for the fully bio-based hydrogel synthesized by Duquette et al., whose copper removal was 30.2 mg/g and nickel removal was reported to be 17.6 mg/g at a starting concentration of 100 mg/L [22].

The removal capacities of the AA/AM hydrogel under non-competitive conditions were similar to those reported in the literature for other synthetic hydrogels, and higher than those reported for bio-based hydrogels [22, 38, 45].

4. Conclusions

Previous hydrogel studies report on the use of foaming agents and foam stabilizers to increase swelling capacity, however, there has not been a study systematically comparing the effect of structure on multiple properties of hydrogels. This paper reported the effect of a foaming agent and foam stabilizer on the physical properties, swelling capacity and ion removal of acrylic acid/acrylamide hydrogels. There was a significant difference between the swelling capacity of the BH, FAH, and FAFSH hydrogels with the FAFSH samples having the highest. Additionally, the 24-hour distilled water rinse had a significant, positive effect on the swelling capacity. The distilled water rinse did not alter the chemical composition of the network, but it did change the surface of the hydrogel granules. While the regenerated hydrogel had an increased swelling capacity, it did not have a significantly different ion removal capacity. The FAFSH and FAH did not display a significant difference in their ion removal capacity. However, they both had a significantly higher ion removal capacity than the BH. Under competitive conditions, the order of preference for the removal of ions was Cd> Cu> Ni for all three structures. This work proves that the use of a foaming agent not only increases the swelling capacity of acrylic acid/acrylamide hydrogels, but also increases their heavy metal removal capacity. Additionally, the use of a rinse to remove unreacted monomers increased the swelling capacity of the hydrogels while retaining the heavy metal removal capacity. The porous foam structure can be applied to other hydrogels, such as bio-based hydrogels, to help enhance swelling capacity and contaminant removal.

Acknowledgements

The Natural Sciences and Engineering Research Council of Canada, Canada Graduate Scholarships—Master's Program (NSERC CGSM), the Fonds de Recherche Nature et Technology (FRQNT) and the Research Center for High Performance Polymer and Composite Systems (CREPEC) are acknowledged for their financial support.

References

[1] R. Singh, N. Gautam, A. Mishra, R. Gupta, Heavy metals and living systems: An overview, Indian journal of pharmacology, 43, 3 (2011), 246.
[2] X. Long, X. Yang, W. Ni, Current status and perspective on phytoremediation of heavy metal polluted soils, Journal of Applied Ecology, 13 (2002), 757-762.
[3] L. Järup, Hazards of heavy metal contamination, British Medical Bulletin, 68, 1 (2003), 167-182.doi: 10.1093/bmb/ldg032.
[4] T. McIntyre, Phytoremediation of heavy metals from soils, Phytoremediation (2003), 97-123.
[5] EPA *2018 Edition of the Drinking Water Standards and Health Advisories Tables*. United States Environmental Protection Agency City, 2018.
[6] WHO *Wastewater use in agriculture*. World Health Organization, City, 2006.
[7] K. Seidal, N. Jörgensen, C.-G. Elinder, B. Sjögren, M. Vahter, Fatal cadmium-induced pneumonitis, Scandinavian journal of work, environment & health (1993), 429-431.
[8] J. Y. Barbee Jr, T. Prince, Acute respiratory distress syndrome in a welder exposed to metal fumes, Southern Medical Journal, 92, 5 (1999), 510-512.
[9] K. Das, S. Das, S. Dhundasi, Nickel, its adverse health effects & oxidative stress, Indian journal of medical research, 128, 4 (2008), 412.
[10] G. G. Stavropoulos, A. A. Zabaniotou, Minimizing activated carbons production cost, Fuel Processing Technology, 90, 7 (2009), 952-957.doi: 10.1016/j.fuproc.2009.04.002.
[11] G. Rorrer, J. Way *Chitosan beeds to remove heavy metal from wastewater*. Dalwoo-ChitoSan, City, 2002.
[12] R. Virta, USGS Minerals Information, US Geological Survey Mineral Commodity Summary 2000.
[13] S. M. Jasinski, USGS Minerals Information, US Geological Survey Mineral Commodity Summary 2001.
[14] S. K. Srivastava, A. K. Singh, A. Sharma, Studies on the uptake of lead and zinc by lignin obtained from black liquor – a paper industry waste material, Environmental Technology, 15, 4 (1994), 353-361.doi: 10.1080/09593339409385438.
[15] S. Babel, T. A. Kurniawan, Low-cost adsorbents for heavy metals uptake from contaminated water: a review, Journal of Hazardous Materials, 97, 1 (2003), 219-243.doi: 10.1016/S0304-3894(02)00263-7.
[16] A. P. Lim, A. Z. Aris, A review on economically adsorbents on heavy metals removal in water and wastewater, Reviews in Environmental Science and Bio/Technology, 13, 2 (2014), 163-181.doi: 10.1007/s11157-013-9330-2.
[17] T. Javanbakht, A. Bérard, J. R. Tavares, Polyethylene glycol and poly(vinyl alcohol) hydrogels treated with photo-initiated chemical vapor deposition, Canadian Journal of Chemistry, 94, 9 (2016), 744-750.doi: 10.1139/cjc-2016-0229.
[18] H. Kaşgöz, S. Özgümüş, M. Orbay, Modified polyacrylamide hydrogels and their application in removal of heavy metal ions, Polymer, 44, 6 (2003), 1785-1793.doi: 10.1016/S0032-3861(03)00033-8.
[19] N. Ni, D. Duquette, M.-J. Dumont, Synthesis and characterization of zein-based cryogels and their potential as diesel fuel absorbent, European Polymer Journal, 91 (2017), 420-428.doi: https://doi.org/10.1016/j.eurpolymj.2017.04.031.
[20] B. Wattie, M.-J. Dumont, M. Lefsrud, Synthesis and Properties Modified Feather Keratin-Based Motor Oil Sorbing Cryogels with High Oil Holding Capacity, Journal of Polymers and the Environment (2016), 1-7.doi: https://doi.org/10.1007/s10924-016-0919-8.
[21] N. Ni, D. Zhang, M.-J. Dumont, Synthesis and characterization of zein-based superabsorbent hydrogels and their potential as heavy metal ion chelators, Polymer Bulletin (2017), 1-15.doi: https://doi.org/10.1007/s00289-017-2017-z.
[22] D. Duquette, C. Nzediegwu, G. Portillo-Perez, M.-J. Dumont, S. Prasher, Eco-Friendly Synthesis of Hydrogels from Starch, Citric Acid, and Itaconic Acid: Swelling Capacity and Metal Chelation Properties, Starch - Stärke, n/a, n/a (2019), 1900008.doi: https://doi.org/10.1002/star.201900008.

[23] L. A. Shah, M. Khan, R. Javed, M. Sayed, M. S. Khan, A. Khan, M. Ullah, Superabsorbent polymer hydrogels with good thermal and mechanical properties for removal of selected heavy metal ions, Journal of Cleaner Production, 201 (2018), 78-87.doi: https://doi.org/10.1016/j.jclepro.2018.08.035.
[24] D. L. Elbert, Liquid–liquid two-phase systems for the production of porous hydrogels and hydrogel microspheres for biomedical applications: a tutorial review, Acta biomaterialia, 7, 1 (2011), 31-56.
[25] K. Kabiri, H. Omidian, S. Hashemi, M. Zohuriaan-Mehr, Synthesis of fast-swelling superabsorbent hydrogels: effect of crosslinker type and concentration on porosity and absorption rate, European Polymer Journal, 39, 7 (2003), 1341-1348.
[26] E. M. Ahmed, Hydrogel: Preparation, characterization, and applications: A review, Journal of Advanced Research, 6, 2 (2015), 105-121.doi: https://doi.org/10.1016/j.jare.2013.07.006.
[27] G. Sennakesavan, M. Mostakhdemin, L. K. Dkhar, A. Seyfoddin, S. J. Fatihhi, Acrylic acid/acrylamide based hydrogels and its properties - A review, Polymer Degradation and Stability, 180 (2020), 109308.doi: https://doi.org/10.1016/j.polymdegradstab.2020.109308.
[28] N. Adnan, S. Ghazali, S. Jamari, Utilization of NaHCO3 as Foam Additive in Synthesis of Superporous Hydrogels, Materials Today: Proceedings, 17 (2019), 995-1000.doi: 10.1016/j.matpr.2019.06.497.
[29] L. Shu Qing, N. Adnan, S. Ghazali, N. Noordin, Effect of gas foaming and porosigen techniques on the properties of superporous hydrogels, Materials Today: Proceedings, 5, 10, Part 2 (2018), 21841-21848.doi: https://doi.org/10.1016/j.matpr.2018.07.040.
[30] G. Craciun, D. Ighigeanu, E. Manaila, M. D. Stelescu, Synthesis and characterization of poly (acrylamide-co-acrylic acid) flocculant obtained by electron beam irradiation, Materials Research, 18 (2015), 984-993.
[31] R. S. Tomar, I. Gupta, R. Singhal, A. K. Nagpal, Synthesis of Poly (Acrylamide-co-Acrylic Acid) based Superabsorbent Hydrogels: Study of Network Parameters and Swelling Behaviour, Polymer-Plastics Technology and Engineering, 46, 5 (2007), 481-488.doi: 10.1080/03602550701297095.
[32] A. Rashidzadeh, A. Olad, Slow-released NPK fertilizer encapsulated by NaAlg-g-poly(AA-co-AAm)/MMT superabsorbent nanocomposite, Carbohydrate Polymers, 114 (2014), 269-278.doi: https://doi.org/10.1016/j.carbpol.2014.08.010.
[33] P. Menter *Acrylamide Polymerization - A Practical Approach*. City.
[34] R. A. Gemeinhart, H. Park, K. Park, Pore structure of superporous hydrogels, Polymers for advanced technologies, 11, 8-12 (2000), 617-625.
[35] H. Chavda, C. Patel, Effect of crosslinker concentration on characteristics of superporous hydrogel, International journal of pharmaceutical investigation, 1, 1 (2011), 17.
[36] A. Ciurzynska, A. Lenart, Freeze-drying-application in food processing and biotechnology-a review, Polish Journal of Food and Nutrition Sciences, 61, 3 (2011).
[37] W.-M. Cheng, X.-M. Hu, Y.-Y. Zhao, M.-Y. Wu, Z.-X. Hu, X.-T. Yu, Preparation and swelling properties of poly(acrylic acid-co-acrylamide) composite hydrogels, e-Polymers, 17, 1 (2017), 95-106.doi: doi:10.1515/epoly-2016-0250.
[38] E. Orozco-Guareño, F. Santiago-Gutiérrez, J. L. Morán-Quiroz, S. L. Hernandez-Olmos, V. Soto, W. d. l. Cruz, R. Manríquez, S. Gomez-Salazar, Removal of Cu(II) ions from aqueous streams using poly(acrylic acid-co-acrylamide) hydrogels, Journal of Colloid and Interface Science, 349, 2 (2010), 583-593.doi: https://doi.org/10.1016/j.jcis.2010.05.048.
[39] S. Nesrinne, A. Djamel, Synthesis, characterization and rheological behavior of pH sensitive poly(acrylamide-co-acrylic acid) hydrogels, Arabian Journal of Chemistry, 10, 4 (2017), 539-547.doi: https://doi.org/10.1016/j.arabjc.2013.11.027.
[40] B. Işık, Swelling behavior and determination of diffusion characteristics of acrylamide–acrylic acid hydrogels, Journal of Applied Polymer Science, 91, 2 (2004), 1289-1293.doi: https://doi.org/10.1002/app.13270.
[41] W. Shi, M.-J. Dumont, E. B. Ly, Synthesis and properties of canola protein-based superabsorbent hydrogels, European Polymer Journal, 54 (2014), 172-180.doi: https://doi.org/10.1016/j.eurpolymj.2014.03.007.

[42] N. V. Gupta, H. Shivakumar, Investigation of swelling behavior and mechanical properties of a pH-sensitive superporous hydrogel composite, Iranian journal of pharmaceutical research: IJPR, 11, 2 (2012), 481.
[43] Y. Bao, J. Ma, N. Li, Synthesis and swelling behaviors of sodium carboxymethyl cellulose-g-poly(AA-co-AM-co-AMPS)/MMT superabsorbent hydrogel, Carbohydrate Polymers, 84, 1 (2011), 76-82.doi: https://doi.org/10.1016/j.carbpol.2010.10.061.
[44] O. B. Akpor, G. O. Ohiobor, D. Olaolu, Heavy metal pollutants in wastewater effluents: sources, effects and remediation, Advances in Bioscience and Bioengineering, 2, 4 (2014), 37-43.
[45] U. Yildiz, Ö. F. Kemik, B. Hazer, The removal of heavy metal ions from aqueous solutions by novel pH-sensitive hydrogels, Journal of Hazardous Materials, 183, 1–3 (2010), 521-532.doi: https://doi.org/10.1016/j.jhazmat.2010.07.055.
[46] J. R. Rangel-Mendez, R. Monroy-Zepeda, E. Leyva-Ramos, P. E. Diaz-Flores, K. Shirai, Chitosan selectivity for removing cadmium (II), copper (II), and lead (II) from aqueous phase: pH and organic matter effect, Journal of Hazardous Materials, 162, 1 (2009), 503-511.doi: https://doi.org/10.1016/j.jhazmat.2008.05.073.
[47] E. Jafarigol, R. Afshar Ghotli, A. Hajipour, H. Pahlevani, M. Baghban Salehi, Tough dual-network GAMAAX hydrogel for the efficient removal of cadmium and nickle ions in wastewater treatment applications, Journal of Industrial and Engineering Chemistry, 94 (2021), 352-360.doi: https://doi.org/10.1016/j.jiec.2020.11.006.
[48] P. C. Gomes, M. P. F. Fontes, A. G. da Silva, E. de S. Mendonça, A. R. Netto, Selectivity Sequence and Competitive Adsorption of Heavy Metals by Brazilian Soils, Soil Science Society of America Journal, 65, 4 (2001), 1115-1121.doi: https://doi.org/10.2136/sssaj2001.6541115x.
[49] A. Ghaee, M. Shariaty-Niassar, J. Barzin, A. Zarghan, Adsorption of copper and nickel ions on macroporous chitosan membrane: Equilibrium study, Applied Surface Science, 258, 19 (2012), 7732-7743.doi: https://doi.org/10.1016/j.apsusc.2012.04.131.
[50] A. T. Paulino, F. A. Minasse, M. R. Guilherme, A. V. Reis, E. C. Muniz, J. Nozaki, Novel adsorbent based on silkworm chrysalides for removal of heavy metals from wastewaters, J Colloid Interface Sci, 301, 2 (2006), 479-487.doi: 10.1016/j.jcis.2006.05.032.
[51] X.-J. Ju, S.-B. Zhang, M.-Y. Zhou, R. Xie, L. Yang, L.-Y. Chu, Novel heavy-metal adsorption material: ion-recognition P (NIPAM-co-BCAm) hydrogels for removal of lead (II) ions, Journal of hazardous materials, 167, 1-3 (2009), 114-118.
[52] M. C. I. M. Amin, N. Ahmad, N. Halib, I. Ahmad, Synthesis and characterization of thermo-and pH-responsive bacterial cellulose/acrylic acid hydrogels for drug delivery, Carbohydrate Polymers, 88, 2 (2012), 465-473.
[53] J. Yang, Y. Fang, C. Bai, D. Hu, Y. Zhang, CuS-poly (N-isopropylacrylamide-co-acrylic acid) composite microspheres with patterned surface structures: Preparation and characterization, Chinese Science Bulletin, 49, 19 (2004), 2026-2032.
[54] S. Sun, P. Wu, A one-step strategy for thermal-and pH-responsive graphene oxide interpenetrating polymer hydrogel networks, Journal of Materials Chemistry, 21, 12 (2011), 4095-4097.
[55] G. Güçlü, E. Al, S. Emik, T. B. İyim, S. Özgümüş, M. Özyürek, Removal of Cu2+ and Pb2+ ions from aqueous solutions by starch-graft-acrylic acid/montmorillonite superabsorbent nanocomposite hydrogels, Polymer Bulletin, 65, 4 (2010), 333-346.doi: 10.1007/s00289-009-0217-x.

Figure Captions

Figure 1: Mechanism of synthesis of acrylic acid/acrylamide hydrogel

Figure 2: a) base hydrogel b) foaming agent hydrogel c) foaming agent, foam stabilized hydrogel

Figure 3: SEM images 50 micrometer scale a) BH b) FAH c) FAFSH d) RBH e) RFAH f) RFAFSH

Figure 4: Swelling capacity of oven dried, foaming agent, foam stabilized hydrogels with 20 wt% initiator

Figure 5: Swelling capacity of foaming agent, foam stabilized hydrogels with varying initiator content and drying methods

Figure 6: Swelling dynamics of acrylic acid/acrylamide hydrogel structures

Figure 7:24 Hour Hydrogel Original and Regenerated Swelling Capacity in Distilled Water

Figure 8a: Swelling capacity of oven-dried hydrogels at varying pH

Figure 8b: Swelling capacity of regenerated oven dried hydrogels at varying pH

Figure 9: Reusability of oven-dried hydrogels

Figure 10:24-hour heavy metal removal under non-competitive conditions

Figure 11:24-hour heavy metal removal competitive conditions

Tables

Table 1: BET Results

Table 2: Hydrogel Formulations

Table 3: 24 hour swelling capacity of hydrogel structures

Table 4: Swelling capacity of novel acrylic acid hydrogels